ELSEVIER

Active Control Law Design for Flutter/LCO Suppression Based on Reduced Order Model Method

Chen Gang*, Li Yueming,Yan Guirong

MOE Key Laboratory for Strength & Vibration, School of Aerospace , Xi'an Jiaotong University, Xi'an, 710049, China

Abstract

Active stability augmentation system is an attractive and promising technology to suppress flutter and limit cycle oscillation (LCO). In order to design a good active control law, the control plant model with low order and high accuracy must be provided, which is one of the most important key points. The traditional model is based on low fidelity aerodynamics model such as panel method, which is unsuitable for transonic flight regime. The physics-based high fidelity tools, reduced order model (ROM) and CFD/CSD coupled aeroservoelastic solver are used to design the active control law. The Volterra/ROM is applied to constructing the low order state space model for the nonlinear unsteady aerodynamics and static output feedback method is used to active control law design. The detail of the new method is demonstrated by the Goland+ wing/store system. The simulation results show that the effectiveness of the designed active augmentation system, which can suppress the flutter and LCO successfully.

Keywords: limit cycle oscillation; aeroelasticity; reduced order model; active control law; static output feedback

1. Introduction

Flutter and limit cycle oscillation (LCO) are the major nonlinear dynamic aeroelastic unstable phenomena and very dangerous to aircraft structure. Recently reduced order models (ROM) based on physics-based high fidelity model for fast prediction of nonlinear aeroelastic response were investigated. The aeroelastic response can be quickly obtained through ROM，which can still capture the physical characteristics of the complex nonlinear aeroelastic system[1]. Different approaches for reduced-order modeling of aerodynamic systems were proposed, including linearization about a nonlinear steady-state flow data-driven model such as Volterra theory of nonlinear systems[2-3] and linear model fitting auto-regressive and moving average (ARMA) model[4], representation of the aerodynamic system in terms of its eigenmodes such as harmony balance (HB) and proper orthogonal decomposition (POD) method[5-6], and representation of the nonlinear aerodynamic system using the nonlinear dynamic theory[7-8].

Traditional active flutter controller is designed based on linear aerodynamic theory such as the panel method, which is a low accurate and low fidelity aerodynamic model. The low fidelity model cannot predict the strong aerodynamic nonlinearity very well, such as shock wave in transonic regime[1,11]. The aerodynamic data computed in frequency domain need to be transformed into time domain for constructing aeroservoelastic model by rational function approximation, which is a tedious work and also requires good experience and knowledge about the aeroelastic system[12-14]. Although ROM had been widely used to investigate the aeroelastic phenomenon in recent years, it is seldom to be used to design the active flutter/LCO controller in aeroservoelasticity community, even for a three-dimensional wing. Volterra/ROM had been applied to designing active flutter suppressing controller for two-freedom aeroelastic system such as airfoil[11] and BACT wing[13] .

This article proposes a new active flutter/LCO control law design method based on Volterra/ROM combined with the CFD/CSD coupled aeroservoelastic solver. The Volterra/ROM is used to construct the aeroelastic state equation model and then the static output feedback control theory is used to design the active control law. Finally the developed CFD/CSD coupled aeroservoelastic solver can be used to evaluate the performance of the active controller. The Goland+

wing/store aeroelastic system is applied to demonstrating the whole procedure.

2. Volterra/ROM

2.1. Volterra series

The Volterra theory represents the input-output relation of a nonlinear time-invariant system. It states that the response of a nonlinear system to an arbitrary input can be evaluated by multi-dimensional convolution integrals, each of which is associated with an internal kernel function. For a nonlinear system, the response $y(n)$ to an arbitrary input signal $u(n)$ can be evaluated by multi-dimensional convolution integrals such as

$$y(n) = h_0 + \sum_{k_1=0}^{n} h_1(n-k_1)u(k_1) +$$

$$\sum_{k_1=0}^{n}\sum_{k_2=0}^{n} h_2(n-k_1, n-k_2)u(k_1)u(k_2) + \cdots +$$

$$\sum_{k_1}^{n}\sum_{k_2}^{n}\cdots\sum_{k_m}^{n} h_m(n-k_1, n-k_2, \cdots, n-k_m) \cdot$$

$$u(k_1)u(k_2)\cdots u(k_m) + \cdots \qquad (1)$$

where n is the discrete-time variable, h_0 the steady state response, and $h_m(n-k_1, n-k_2, \cdots, n-k_m)$ the Volterra kernel of the system.

A central issue in the application of the Volterra theory is the identification of these kernel functions. The use of Volterra theory for modeling aerodynamic systems（Volterra/ROM）was first suggested by W. A. Silva, who implemented a direct kernel identification method based on the system response to impulse inputs[2]. The nonlinear Navier-Stokes (N-S) equations can be considered weakly nonlinear and can be accurately represented by a truncated second-order Volterra series[1-2,11]. This is based on the fact that highly nonlinear phenomena have negligible impact on the net effect of various responses under the conditions of small perturbation excitations. D. E. Raveh further pointed out that the step input is better than the impulse input to characterize the nonlinear aerodynamic system[10]. The use of steps in a first-order ROM or in a second-order ROM with a limited number of retained kernel components results in more accurate prediction. For linear problems such as flutter or gust perturbation, the components of second kernel $h_2(n,n)$ are much smaller than $h_1(n)$ and also vanish to zero very quickly, so the system response can be accurately predicted by using only the first-order step-based ROM kernel which includes the linearized nonlinear effect[1,5-7].

Define the unit step input signal as

$$\xi(n) = \begin{cases} 1 & n \geq 0 \\ 0 & n < 0 \end{cases} \qquad (2)$$

Compute the unit step response $s(n)$ by the CFD solver, and the first-order kernel for unit step response is

$$h_1(i) = \begin{cases} s(0) & i = 0 \\ s(i) - s(i-1) & i \geq 1 \end{cases} \qquad (3)$$

For dynamic aeroelastic response prediction, the steady state response of the system h_0 can be subtracted from the system response. Retaining the first-order term of Eq.(1) and substituting Eq.(3) into it, the system response to arbitrary input can be obtained:

$$y(n) = u(0)s(n) + \sum_{i=1}^{n} s(n-i)[u(i) - u(i-1)] =$$

$$u(0)s(n) + \sum_{i=1}^{n} s(n-i)\dot{u}(i)\Delta t \qquad (4)$$

2.2. Eigensystem realization algorithm (ERA)

The analysis of the convolution of the derivative of the step response method shows that by approximating the response with the derivative of the step response, more nonlinear effect is included in the predicted response. But Eq.(4) is not suitable for system analysis such as stability analysis or controller design. The goal of ERA is to transform the Volterra series into the discrete state space-model which is very convenient for control analysis. The discrete state space equation of unsteady aerodynamics realized by ERA method is[10]

$$\left.\begin{array}{l} \boldsymbol{x}_A[n+1] = \boldsymbol{A}_A\boldsymbol{x}_A[n] + \boldsymbol{B}_A\boldsymbol{\xi}[n] \\ \boldsymbol{F}_A[n] = \boldsymbol{C}_A\boldsymbol{x}_A[n] + \boldsymbol{D}_A\boldsymbol{\xi}[n] \end{array}\right\} \qquad (5)$$

where $\boldsymbol{x}_A[n]$ is the state variables of unsteady aerodynamics, $\boldsymbol{\xi}[n]$ the general displacement of structure, $\boldsymbol{F}_A[n]$ the general mode aerodynamics(GAF), and $\boldsymbol{A}_A$, $\boldsymbol{B}_A$, $\boldsymbol{C}_A$ and $\boldsymbol{D}_A$ are the control matrix, input matrix, output matrix and feedforward matrix of the state space model whose dimension is determined by ERA method autonomously.

The zero state impulse response of a linear time-invariant discrete system is given by a function known as Markov parameter:

$$\boldsymbol{h}(i) = \boldsymbol{s}(i) - \boldsymbol{s}(i-1) = \boldsymbol{C}_A\boldsymbol{A}_A^{i-1}\boldsymbol{B}_A \qquad (6)$$

Fortunately for aeroelastic system, $h(i)$ is just the identified first-order Volterra kernels from Eq.(3), whose order is $M \times L$. M is the number of the modeled structure modes and L the number of structure modes used to compute step response. In order to solve the state space matrix $\boldsymbol{A}_A$, $\boldsymbol{B}_A$, $\boldsymbol{C}_A$ and $\boldsymbol{D}_A$, the Hankel matrix is formed by windowing the derivative of the step response data:

$$\boldsymbol{H}(k-1) = \begin{bmatrix} h(k) & h(k+1) & \cdots & h(k+\beta-1) \\ h(k+1) & h(k+2) & \cdots & h(k+\beta) \\ h(k+2) & h(k+3) & \cdots & h(k+\beta+1) \\ \vdots & \vdots & & \vdots \\ h(k+\alpha-1) & h(k+\alpha) & \cdots & h(k+\alpha+\beta+1) \end{bmatrix} \qquad (7)$$

where α is the number of time steps used to shift the data window and β the total size of data window. They are the appropriate constants selected according to the Volterra kernel signals. The ERA method eliminates redundant data by using a singular value decomposition (SVD) of $\boldsymbol{H}(0)$

$$\boldsymbol{H}(0) = \boldsymbol{U}\,\boldsymbol{\Sigma}\,\boldsymbol{V}^{\mathrm{T}} \qquad (8)$$

Suppose

$$\left.\begin{array}{l}\boldsymbol{E}_M = \begin{bmatrix} \boldsymbol{I}_M & \boldsymbol{0}_M & \cdots & \boldsymbol{0}_M \end{bmatrix}^{\mathrm{T}} \quad (M \times \alpha M \text{ order}) \\[2mm] \boldsymbol{E}_L = \begin{bmatrix} \boldsymbol{I}_L & \boldsymbol{0}_L & \cdots & \boldsymbol{0}_L \end{bmatrix}^{\mathrm{T}} \quad (L \times \beta L \text{ order}) \end{array}\right\}$$

$$(9)$$

where $\boldsymbol{0}_M$ and $\boldsymbol{0}_L$ are the null matrices of order M and L respectively , and $\boldsymbol{I}_M$ and $\boldsymbol{I}_L$ the identity matrices of order M and L. Then the state-space realization can be obtained as follows:

$$\left.\begin{array}{l}\boldsymbol{A}_A = \boldsymbol{\Sigma}^{-1/2}\boldsymbol{U}^{\mathrm{T}}\boldsymbol{H}(1)\boldsymbol{V}\,\boldsymbol{\Sigma}^{-1/2} \\[2mm] \boldsymbol{B}_A = \boldsymbol{\Sigma}^{1/2}\boldsymbol{V}^{\mathrm{T}}\boldsymbol{E}_L \\[2mm] \boldsymbol{C}_A = \boldsymbol{E}_M^{\mathrm{T}}\boldsymbol{U}\,\boldsymbol{\Sigma}^{1/2} \\[2mm] \boldsymbol{D}_A = \boldsymbol{h}(0) \end{array}\right\} \qquad (10)$$

2.3. Aeroservoelastic state space equation

The purpose of constructing ROM is to create state space equation of the aeroelastic system. The structure equation is

$$\boldsymbol{M}_s\ddot{\boldsymbol{\xi}} + \boldsymbol{C}_s\dot{\boldsymbol{\xi}} + \boldsymbol{K}_s\boldsymbol{\xi} = q\boldsymbol{F}_A(t) \qquad (11)$$

where q is dynamic pressure. Suppose the transform

function of the actuator is

$$\frac{\beta(s)}{\beta_{\mathrm{c}}(s)} = \frac{k_0\omega_0^2}{s^2 + 2\zeta\omega_0 s + \omega_0^2} \qquad (12)$$

where β is deflection of control surface，β_{c} the command of control surface，k_0 the proportional coefficient，ω_0 fixed frequency and ζ the damping of the actuator. Transform Eq.(12) from frequency domain into time domain and combine with Eq.(11), then the structure-servo couple system is obtained:

$$\boldsymbol{M}_{\mathrm{sc}}\ddot{\boldsymbol{\xi}}_{\mathrm{sc}} + \boldsymbol{C}_{\mathrm{sc}}\dot{\boldsymbol{\xi}}_{\mathrm{sc}} + \boldsymbol{K}_{\mathrm{sc}}\boldsymbol{\xi}_{\mathrm{sc}} = q\boldsymbol{F}_A(t) + \begin{bmatrix} 0 & 0 & k_0\omega_0^2 \end{bmatrix}^{\mathrm{T}}\boldsymbol{\beta}_{\mathrm{c}}$$

$$\boldsymbol{\xi}_{\mathrm{sc}} = \begin{bmatrix} \xi & \beta \end{bmatrix}^{\mathrm{T}}, \quad \boldsymbol{M}_{\mathrm{sc}} = \begin{bmatrix} \boldsymbol{M}_s & \boldsymbol{0} \\ \boldsymbol{0} & 1 \end{bmatrix}$$

$$\boldsymbol{C}_{\mathrm{sc}} = \begin{bmatrix} \boldsymbol{C}_s & \boldsymbol{0} \\ \boldsymbol{0} & 2\zeta\omega_0 \end{bmatrix}, \quad \boldsymbol{K}_{\mathrm{sc}} = \begin{bmatrix} \boldsymbol{K}_s & \boldsymbol{0} \\ \boldsymbol{0} & \omega_0^2 \end{bmatrix}. \quad (13)$$

Let $\boldsymbol{x}_s(t)=[\boldsymbol{\xi}_{\mathrm{sc}}\ \ \dot{\boldsymbol{\xi}}_{\mathrm{sc}}]^{\mathrm{T}}$ and rewrite Eq.(13) as state space equation

$$\left.\begin{array}{l}\dot{\boldsymbol{x}}_s(t) = \boldsymbol{A}_s\boldsymbol{x}_s(t) + q\boldsymbol{B}_s\boldsymbol{F}_A(t) + \boldsymbol{B}_C\boldsymbol{\beta}_{\mathrm{c}} \\[2mm] \boldsymbol{\xi}(t) = \boldsymbol{C}_s\boldsymbol{x}_s(t) + q\boldsymbol{D}_s\boldsymbol{F}_A(t) \end{array}\right\} \qquad (14)$$

$$\boldsymbol{A}_s = \begin{bmatrix} \boldsymbol{0} & \boldsymbol{1} \\ -\boldsymbol{M}_{\mathrm{sc}}^{-1}\boldsymbol{K}_{\mathrm{sc}} & -\boldsymbol{M}_{\mathrm{sc}}^{-1}\boldsymbol{C}_{\mathrm{sc}} \end{bmatrix}$$

$$\boldsymbol{B}_s = \begin{bmatrix} \boldsymbol{0} \\ \boldsymbol{M}_{\mathrm{sc}}^{-1} \end{bmatrix}, \boldsymbol{C}_s = \boldsymbol{I}, \boldsymbol{D}_s = \boldsymbol{0}$$

Transform it into discrete state space as

$$\left.\begin{array}{l}\boldsymbol{x}_s(n+1) = \bar{\boldsymbol{A}}_s\boldsymbol{x}_s(n) + q\bar{\boldsymbol{B}}_s\boldsymbol{F}_A(n) + \boldsymbol{B}_C\boldsymbol{\beta}_{\mathrm{c}} \\[2mm] \boldsymbol{\xi}(n) = \boldsymbol{C}_s\boldsymbol{x}_s(n) \end{array}\right\} \qquad （15）$$

Combining Eq.(5）and Eq.(15）, the discrete state space aeroservoelastic equation is

$$\left.\begin{array}{l}\begin{bmatrix} \boldsymbol{x}_s(n+1) \\ \boldsymbol{x}_A(n+1) \end{bmatrix} = \begin{bmatrix} \bar{\boldsymbol{A}}_s + q\bar{\boldsymbol{B}}_s\boldsymbol{D}_A\bar{\boldsymbol{C}}_s & q\bar{\boldsymbol{B}}_s\bar{\boldsymbol{C}}_A \\ \boldsymbol{B}_A\bar{\boldsymbol{C}}_s & \boldsymbol{A}_A \end{bmatrix}\begin{bmatrix} \boldsymbol{x}_s(n) \\ \boldsymbol{x}_A(n) \end{bmatrix} + \begin{bmatrix} \bar{\boldsymbol{B}}_C \\ \boldsymbol{0} \end{bmatrix}\boldsymbol{\beta}_{\mathrm{c}} \\[4mm] y(n) = \begin{bmatrix} \boldsymbol{\xi}(n) & \dot{\boldsymbol{\xi}}(n) \end{bmatrix} = \begin{bmatrix} \boldsymbol{I} & \boldsymbol{0} \end{bmatrix}\begin{bmatrix} \boldsymbol{x}_s(n) \\ \boldsymbol{x}_A(n) \end{bmatrix} \end{array}\right\}$$

$$(16)$$

The aeroelastic equation can be obtained by supposing $\bar{\boldsymbol{B}}_C = \boldsymbol{0}$. For active control of aeroelastic system, we need to design a controller to suppress the unstable response. The input of the aeroservoelastic system Eq.(16）is $\boldsymbol{\beta}_{\mathrm{c}}$ and the corresponding output is the structure response such as displacement and velocity. The active control/stability augmentation problem is to design the control law to stabilize the structure response such as flutter or LCO.

2.4. Optimal static output feedback control law design

In most of the practical aeroelastic control problems it is impossible to measure all the states of the system. For example, the state variables for the nonlinear aerodynamics cannot be directly measured. So linear

quadratic regulator (LQR) or linear quadratic Gauss (LQG) controller needs a state observer to estimate these state variables, while the state observer will reduce the robustness of the controller. On the other hand, LQR or LQG controllers are dynamic controllers that have the same order as the assumed plant. Real-time implementation of high-order controllers is also very difficult.

Static output feedback (SOF) controllers are based on direct feedback of the sensor output[15]. Its control gain is constant. Unlike LQR controller, SOF does not assume the availability of all the system states for feedback. It is just assumed that only a few linear combinations of system states are available，which can be directly measured from the sensors. An optimal SOF controller aims to find the feedback gains to optimize a given performance index.

Give an nth-order linear time invariant (LTI) stabilizable system as

$$\left.\begin{array}{l}\dot{x} = Ax + Bu + Dw \\ y = Cx\end{array}\right\} \tag{17}$$

where x is the system states, A the system dynamics matrix in state-space form, u the actuator command and its order is p, B the control actuation matrix, y the sensor measurements and its order is q, C the matrix relating the sensor measurements to the state variables, w zero mean unit intensity white noise process, and D the matrix of noise intensity. Assuming constant gain output feedback of the form is

$$u(t) = -Ky(t) \tag{18}$$

Feedback gains K can be determined to stabilize the closed-loop system and minimize the quadratic performance:

$$J = \frac{1}{2}\int_0^\infty [x^T(t)Qx(t) + u^T(t)Ru(t)]dt \tag{19}$$

The solution to the optimization problem given above is

$$\left.\begin{array}{l}K = R^{-1}B^T P \\ PA + A^T P - PBR^{-1}B^T P + Q = 0\end{array}\right\} \tag{20}$$

where P is the solution of Riccati equation which can be calculated by a variety of iterative algorithms[15].

3. Goland+ Wing/Store System

3.1. Goland+ wing model

The Goland+wing/store model is a variant of the heavy Goland wing developed as a transonic flutter test case by F. E. Eastep, et al.[16]. Based on the original Goland wing, the heavy Goland wing has increased mass to ensure applicability in the transonic regime. The Goland+ wing is rectangular and cantilevered from an infinite midplane. The wing semi-span is 6.096 m and the chord is 1.828 8 m. The thickness-to-chord ratio is 0.04. The elastic axis is located 0.609 6 m from the leading edge. The airfoil section is constant over the spanwise extent of the wing and is chosen to be symmetric. There is a 3.048 m long and 0.127 m diameter cylindrical store with an elliptic nose cone centered on the wing tip. The Goland+ wing/tip store structure is modeled by finite element method with MSC/Nastran in which the wing structure is modeled with twenty box structure beam elements and the tip store is modeled with four integrated mass elements as shown in Fig.1.The first six mode shapes are presented in Fig.2 and the mode frequencies of first six structure modes are 1.705 1, 3.051 6, 9.200, 10.906, 16.271 and 22.861 Hz respectively, which are close to the experimental data[16].
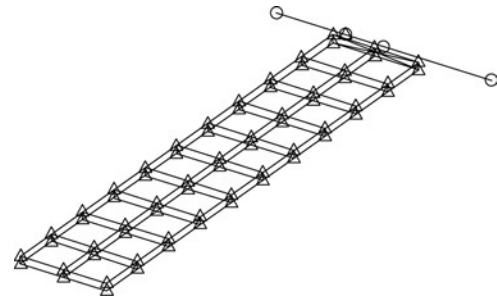

Fig.1   Configuration of Goland+wing/tip store system.

(a) 1.705 1 Hz   (b) 3.051 6 Hz

(c) 9.200 Hz   (d) 10.906 Hz
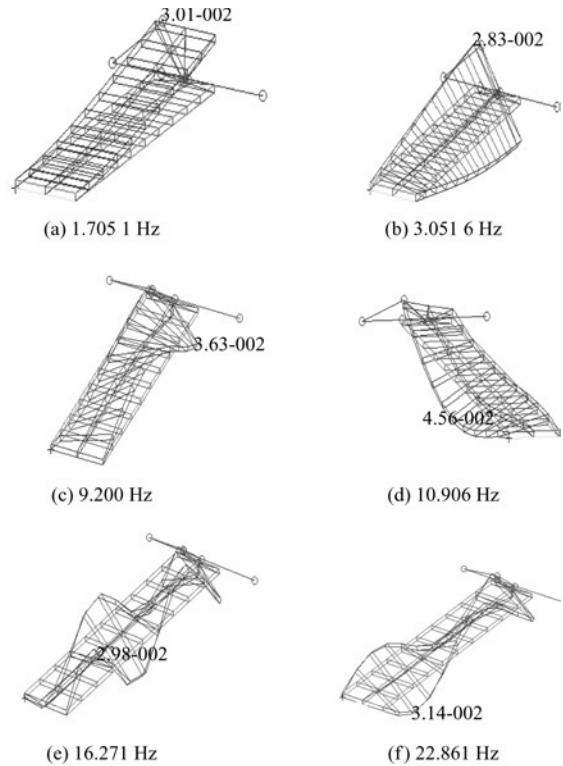
(e) 16.271 Hz   (f) 22.861 Hz

Fig.2   The first six modes of Goland+ wing/store system.

3.2. Flutter/LCO simulation of Goland+wing/store system

The coupled CFD/CSD solver based on Euler/N-S equations and Roe scheme developed by the authors had been used to simulate the aeroelastic phenomena such as flutter and LCO and was validated by NLR 7301 airfoil model, AGARD 44.6 wing and Goland+ wing[6,9,14]. The wing/store system had 0.2 million aerodynamic grid points. Infinite plate spline (IPS) interpolation method is used to deal with the mesh mapping between the flow and structure, and the spring analogy dynamic mesh algorithm applied to the movement of the grids. At Mach number 0.92, the dynamic pressure 34 578 Pa and angle of attack zero, the perturbation velocity 0.1 is given to structure Mode 2. The time step is 0.001 s and it costs nearly 20 h to obtain the LCO.

Figs.3-4 show the time response of each structure mode of the wing/store system and the phase diagram of Mode 1. The amplitude of LCO and the frequency

are very close to the simulation results of Berran's[17] and the difference is no more than 6%. From these results it can be concluded that under these conditions the Goland+ wing/store system is beyond the flutter point. Because of the nonlinear aerodynamics, it will diverge very quickly and then run into the LCO finally. It is required to stabilize the wing/store system for enhancing the flight envelope of aircraft.
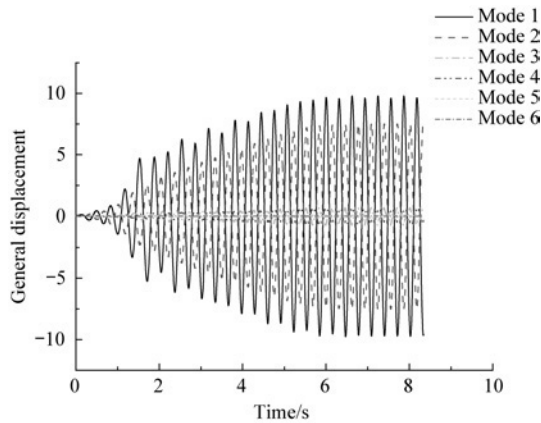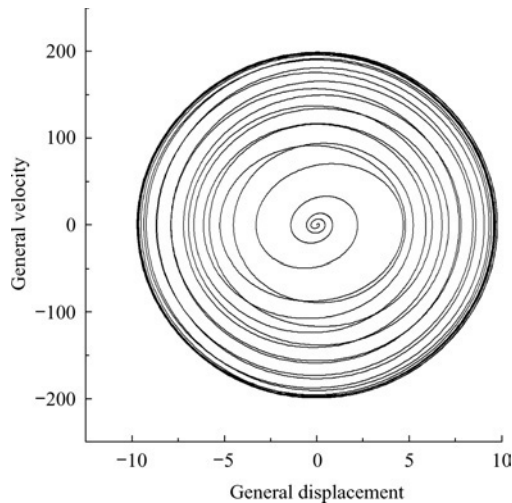

Fig.3   LCO of Goland+ wing.

Fig.4   Phase diagraph of Mode 1.

4. Active Flutter/LCO Suppression Based on Volterra/ROM Method

4.1. Control model construction based on ROM

As a demonstration and shown in Fig.5, one control flap surface with the length 1.13 m and width 0.45 m at the center of the rear edge is used to suppress the divergent wing/store system. Firstly we will construct the Volterra/ROM for Goland+ wing/store system based on the flow condition of Section 3.2. Geographical adaptive fidelity (GAF) algorithm for step response of Mode 1 is computed where the amplitude of structure displacement is 0.01 with the time step 0.000 1 s. The smaller time step can increase the accuracy of the kernel identification. GAF related to struc-

ture Mode 1 is plotted in Fig.6 and then the Volterra kernel of Mode 1 is created according to the Eq.(3). The Volterra kernels of other structure modes can be obtained as the same procedure, including GAF of the control surface which is plotted in Fig.7. In order to show GAF, more than 500 time steps are run. But in fact, the simulation can be stopped when the change of the responses is very small such as about 300 time steps. Then the discrete state space equation of unsteady aerodynamic model can be constructed by the ERA method with $\alpha = 200$ and $\beta = 25$. And then the aeroelastic and aeroservoelatic state space equation was constructed according to method described in Section 2.3.
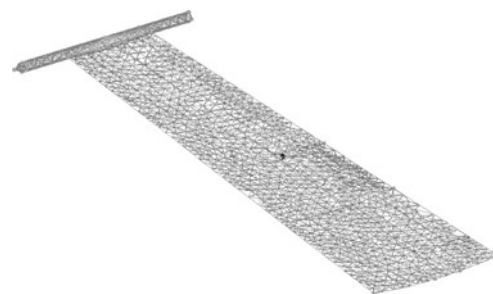

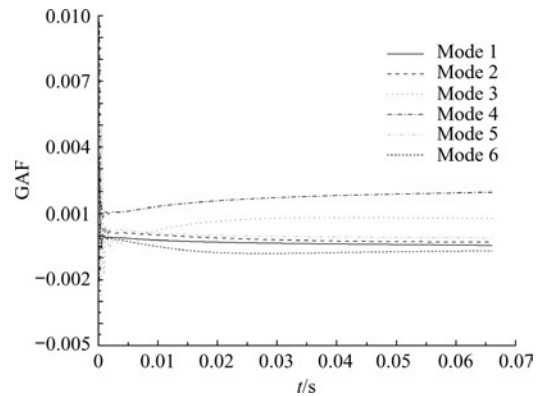Fig.5   Control surface diagram.

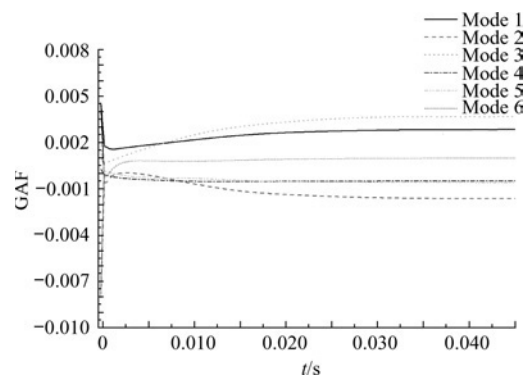Fig.6   GAF for step response of Mode 1.

Fig.7   GAF for step response of control.

Before designing the active control/stability augmentation system, the Volterra/ROM must be evaluated by the CFD/CSD coupled solver. Fig.8 gives the comparison of GAF response of the six structure modes between ROM (dash line) and the coupled solver (solid line, time step=0.001 s) for the first 800

steps. As can be seen, the results are very close, which indicates that ROM model is good enough to present the main aeroelastic behavior of the wing/store system.
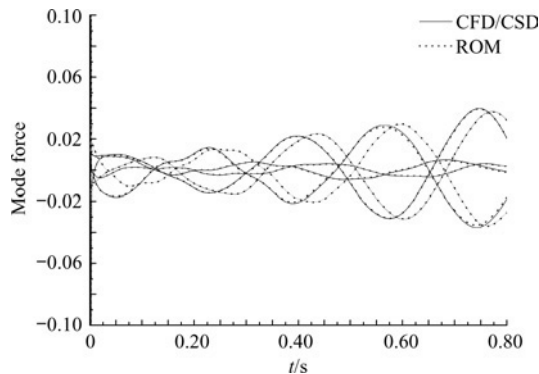

Fig.8   Aeroelastic response of structure.

4.2. Active controller design for flutter suppression

The structure of SOF controller is dependent on the placement of the sensors. Here twist sensors (for torsion), curvature sensors (for bending), the corresponding twist-rate and curvature-rate sensors are used. More additional sensors will lead to progressively more information on higher modes. The velocity of structure mode can be identified from the outputs of the sensors directly, so it can be used as the feedback signals. The formula of the control law can be selected as $\delta = [K_1 \quad K_2 \quad \cdots \quad K_6] [\dot{\xi}_1 \quad \dot{\xi}_2 \quad \cdots \quad \dot{\xi}_6]^T$. From Fig.3, we can find out that the amplitudes of Mode 1 and Mode 2 are among the largest, which means the aeroelastic system is dominated by the torsion and bending deformations. So we just need to identify the output information of the first two structure modes from the sensors and SOF controller can be reduced to second-order.

After selecting the structure of the SOF controller, the MATLAB/SIMULINK is used to design the controller. Let $Q = 0$ and $P = 1$, we could obtain the optimal control gain $K = [0.001, 0.002]$. And then we use the MATLAB/SIMULINK and CFD/CSD coupled solver to simulate the flutter suppression with the time step 0.001 s. In the simulation process, the first two structure initial displacements are −1.4 and 0.9. Fig.9 is the
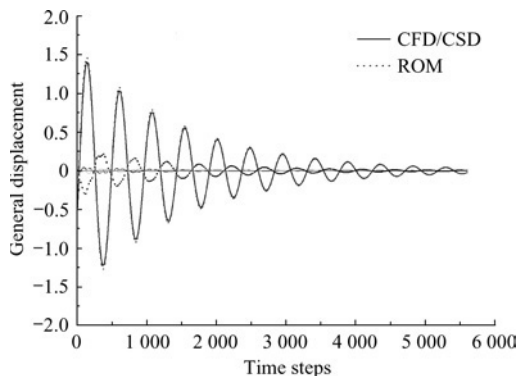
aeroelastic response of the structure, and Fig.10 is the control command of the control surface. It indicates that the unstable wing/store system can be suppressed by the active SOF controller very quickly. And the responses of ROM and coupled solver are very close which give another validation for the accuracy of Volterra/ROM.
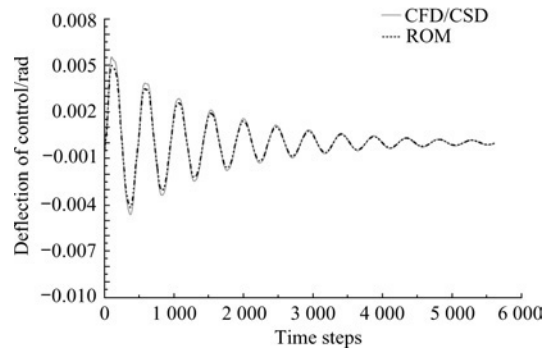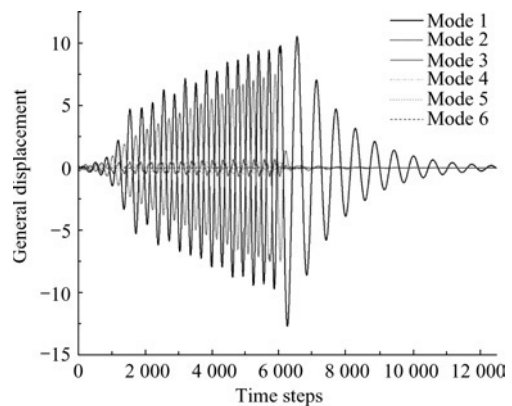

Fig.10   Control surface response.

4.3. LCO simulation with active SOF controller

Volterra/ROM is only suitable for modeling weak nonlinear aeroelasticity such as flutter and gust response. It cannot capture LCO generated by nonlinear aerodynamics. So it cannot be justified directly from the MATLAT/SIMULIN simulation whether the SOF controller designed for flutter suppression can stabilize the LCO or not. But fortunately, CFD/CSD coupled solver can be used to simulate the Goland+ wing/store system with the SOF controller and answer the question.

In order to verify the LCO suppression performance of the SOF controller, the active controller starts at time steps 6 000 when the system runs into LCO. Fig.11 shows the response of the wing structure and control surface. Fig.12 plots the phase diagraph. The simulation shows that the SOF controller can suppress the LCO very quickly. From the view point of control theory, when the control surface switched on, the open aeroelastic system become a closed aeroservoelastic system whose characteristics will change. In physics,
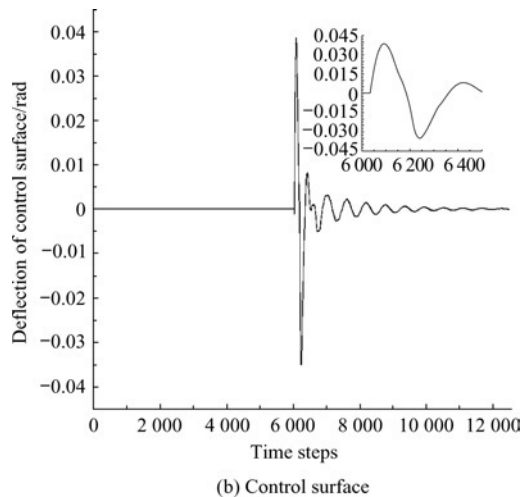

Fig.9   Aeroelastic response with active controller.

(a) Wing structure

(b) Control surface

Fig.11   Response of wing structure and control surface.

(a) Phase diagraph of Mode 1
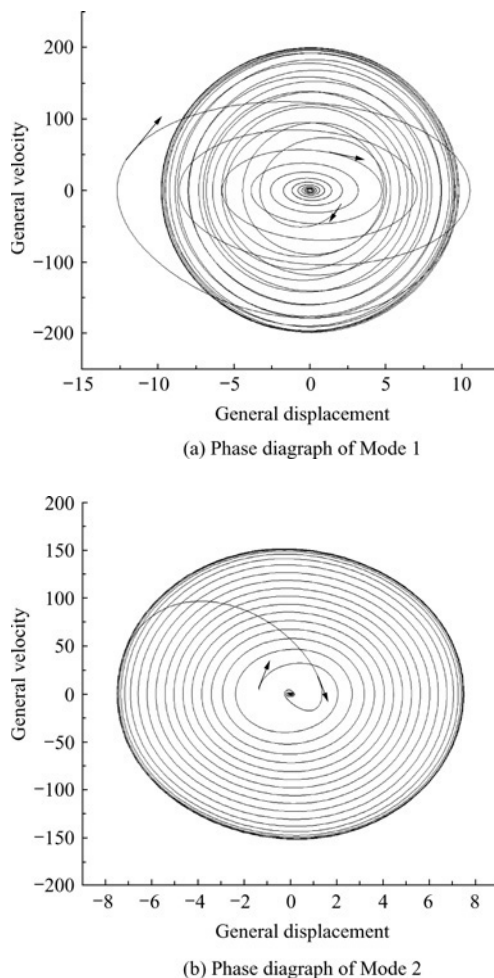

(b) Phase diagraph of Mode 2

Fig.12   Phase diagraphes of Modes 1 and 2.

the movements of the control surface will change the unsteady pressure distribution in the wing/store and then change the vibration response of the aeroelastic system. Especially, it can be found that the phase of the control surface movement is opposite to the phase of the vibration of the wing structure. That is why the

control surface can suppress the LCO and make the structure vibration to zero finally.

From the zoom picture we can see the deflection of flap is also smooth. The largest rate of the movement of the flap at the start of the controller is 0.78 rad/s, which is below the maximum allowable rate 1 rad/s. Although there is little time delay nearly 0.05 s at the start, the deflection of the flap tracked the command very well after nearly 0.1 s. The largest deflection of the control surface is no more than 0.04 and it reduces very quickly to below 0.005 just in several cycles. The smaller control surface defection has little effect on the original rigid body flight dynamic control system. This is very important in synthesizing the flight control system with active control system.

5. Conclusions

(1) We have demonstrated the effectiveness of active control/stability augmentation system based on Volterra/ROM for flutter/LCO suppression of Goland+ wing/store system. The Volttera/ROM combined CFD/CSD coupled solver is a good tool for flutter/LCO suppression system design.

(2) However, as we all know the system identification ROM is based on the dynamic linearization data-driven method with small perturbation, and it cannot capture the strong aerodynamic nonlinearity such as LCO. Therefore, the design of active control/stability augmentation system for LCO suppression will require much more tedious work (e.g. much longer computational time to capture the LCO) than flutter suppression, though the active control/stability augmentation system for flutter suppression can also suppress the LCO in most cases. In order to enhance the efficiency and performance of the controller for LCO, better nonlinear ROM model which can capture LCO directly is required, such as K. J. Badcock's bifurcation ROM.

(3) For the Goland+wing/store case, the bending mode's performance is not as good as the torsion mode, so the optimization of the size of the control surface or more flaps can be considered in further study. Another importance is the synthesis of flight control system and active control system.

References

[1]   Lucia D J, Beran P S, Silva W A. Reduced-order modeling: new approaches for computational physics. Progress in Aerospace Sciences 2004; 40(1): 51-117.

[2]   Silva W A. identification of linear and nonlinear aerodynamic impulse responses using digital filter techniques. AIAA-1997-3712, 1997.

[3]   Wu Z G, Yang C. Volterra series based transonic unsteady aerodynamics modeling. Journal of Beijing University of Aeronautics and Astronautics 2006; 32(4): 373-376. [in Chinese]

[4]   Gupta K K, Voelker L S, Bach C, et al. CFD-based aeroelastic analysis of the X-43 hypersonic flight vehi-

cle. AIAA-2001-712, 2001.

[5]   Hall K C, Thomas J P, Dowell E H. Proper orthogonal decomposition technique for transonic unsteady aerodynamic flows. AIAA Journal 2000; 38(10): 1853-1862.

[6]   Chen G, Li Y M, Yan G R, et al. A fast aeroelastic response prediction method based on proper orthogonal decomposition reduced order model. Journal of Astronautics 2009; 30(5): 1765-1769. [in Chinese]

[7]   Woodgate M A. Badcock K J. Fast prediction of transonic aeroelastic stability and limit cycles. AIAA Journal 2007; 45(6): 1370-1381.

[8]   Thomas J P, Dowell E H, Hall K C. Using automatic differentiation to create a nonlinear reduced order model of a computational fluid dynamic solver. AIAA-2006-7115, 2006.

[9]   Chen G, Li Y M, Yan G R. Nolinear POD reduced order model for limit cycle oscillation predition. AIAA-2010-2726, 2010.

[10] Raveh D E. Reduced-order models for nonlinear unsteady aerodynamics. AIAA Journal 2001; 39(8): 1417-1429.

[11] Marzocca P, Silva W A, Librescu L. Open/closed-loop nonlinear aeroelasticity for airfoils via volterra series approach. AIAA Journal 2004; 42(4): 673-686.

[12] Hu P, Dowell E H. Physics-based identification, modeling and management Infrastructure for aeroelastic limit-cycle oscillations. US Air Force Annual-Structural Dynamics Conference. 2008.

[13] Zhang Z, Xu M, Chen S L. Active flutter control of transonic flapped wing based on CFD/CSD coupling. 7th International Conference on System Simulation and Scientific Computing (ICSC'2008). 2008; 430-435.

[14] Chen G. Active control method of flexible flight vehicle. PhD thesis, Xi'an Jiaotong University, 2008. [in Chinese]

[15] Syrmos V L, Abdallah C T, Dorato P, et al. Static output feedback: a survey. Automatica 1997; 33(2): 125-137.

[16] Eastep F E, Olsen J J. Transonic flutter analysis of a rectangular wing with conventional airfoil sections. AIAA Journal 1980; 18(10): 1159-1164.

[17] Parker G H, Maple R C, Beran P S. Analysis of store effects on limit-cycle oscillation. AIAA-2006-1846, 2006.

Biography:

Chen Gang   Born in 1979, he received B.S., M.S. and Ph.D. degrees from Northwestern Polytechincal University in 2001, 2004 and 2006 respectively, and then worked as a Postdoctor in Xi'an Jiaotong University (XJTU). He obtained the faculty position of XJTU and is now an associate professor of School of Aerospace. His main research interest is aeroservoelasticity, aerodyanmics and flight dynamics.
E-mail: aachengang@mail.xjtu.edu.cn